



VOLUMETRIC, LUMPED AND 2-D NUMERICAL MODELS OF THE MOMOTOMBO RESERVOIR, NICARAGUA

Idalia Araceli Matus Pravia

Nicaraguan Electricity Company

Geochemistry Laboratory

Intersección Pista Juan Pablo II y Prolongación Ave. Bolívar

Managua

NICARAGUA

imatus@enel.gob.ni

ABSTRACT

The production capacity of the Momotombo geothermal field has declined over time when production wells were damaged by scaling and suffered from cooling. The reservoir is characterized by a deep, vertical upflow zone of 280-320°C feeding a shallow horizontal reservoir at 300-500 m depth and 180-240°C temperature. Geothermal fluid was observed on the surface in hot springs and fumaroles. The chloride concentration in most of the production wells has been decreasing because of the incursion of cold water into the reservoir, presumably entering the reservoir by the hot spring conduits. The proven and possible production capacity for 25 years was estimated using the Monte Carlo volumetric method at 20 MW and 50 MW, respectively. The total production data and pressure drawdown were simulated satisfactorily by a one- and two-tank open lumped model. The two-tank open model yielded a reservoir volume in the 4 km³ range, the same as the estimated proven reservoir volume in the Monte Carlo method. The permeability of the lumped model ranged from 75 to 230 mD. A 2D numerical model was developed and calibrated using the code iTOUGH2, allowing for the study of the chloride concentration changes over time. The thin 2D slice could be heated up by 3.3 kg/s of 330°C water. The highest permeability of 340 mD complies well with the inner 230 mD permeability of the lumped model. The results of the simulation indicated that chloride concentration is a good parameter for future studies. Decreases in chloride concentration imply intrusion of low temperature and fresh groundwater into the reservoir. Intrusion of low-temperature groundwater into the reservoir and extensive boiling in the shallow reservoir due to pressure drawdown induced cooling in the reservoir and these are regarded here as the main reasons for the operational problems encountered in the wellfield management.

1. INTRODUCTION

1.1 The Momotombo developmental history

The Momotombo geothermal field is located on the southwest flank of the Cordillera Los Marrabios, on the northern shore of Lake Managua, at the foot of the Momotombo stratovolcano (Figure 1).

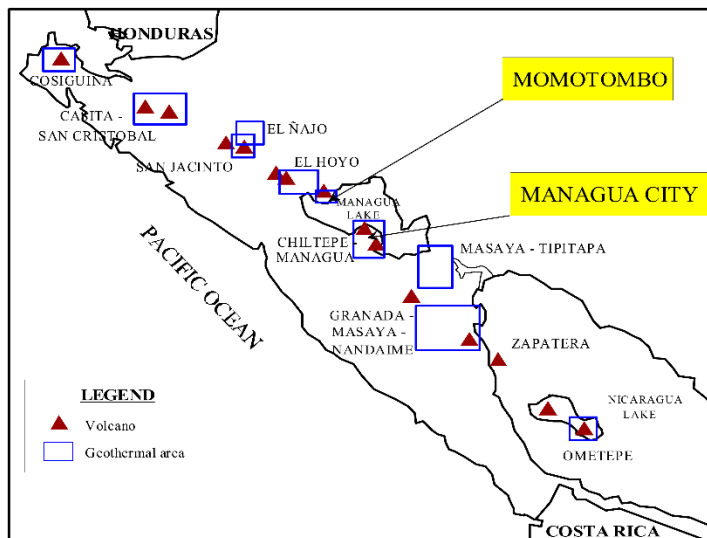


FIGURE 1: Location map of Momotombo (Porrás, 2008)

Momotombo is currently the most intensely studied geothermal field in Nicaragua, with a long production history.

The field began producing electricity in 1983 with an installed capacity of 35 MWe. In 1989, another 35 MWe unit was commissioned. Soon thereafter the increased steam production rate led to downhole scaling and lost enthalpies, mainly due to a decline in well productivity caused by either temperature and pressure drops in the reservoir or scaling in the wellbore and formation. This field's behaviour led to a production history which declined from a short peak of 69 MWe in 1991 to 9 MWe in 1999 (Björnsson, 2008).

During this period, production well output decreased rapidly, showing marked changes in temperature and pressure, paralleled by changes in the consistency and chemistry of the geothermal fluids and the enthalpy (Porrás and Björnsson, 2010). All these changes are attributed to excessive exploitation of the proven resource, low injection volumes, maintenance challenges, and rapid infiltration of cold lake water into the reservoir.

This resource management problem was largely mitigated when Ormat took over field operations, led by mechanical work-overs (acid stimulation, calcite scaling inhibition, full reinjection and drilling of deep wells) in order to recover steam production. In 2002, an organic unit Rankine cycle Ormat Energy Converter (OEC) was commissioned with a 7 MWe installed capacity, increasing the total installed capacity to 77 MWe. Nowadays, the power production in Momotombo power plant has stabilized at 25 MWe.

1.2 Goal of the present study

The main objectives of the present study are:

- 1) To carefully review available literature of Momotombo and identify data sources of value for reservoir engineering studies;
- 2) To collect and plot with time the chloride concentrations history from the Momotombo geothermal production wells to shed light on the nature of the reservoir's outer boundaries;
- 3) To estimate the proven and possible production for 25 years of plant life of the Momotombo geothermal field by using the Monte Carlo volumetric method;
- 4) To calibrate a simple lumped parameter model simulating the reservoir pressure drawdown history and compare this model's properties with the Monte Carlo volumetric method; and
- 5) Study changes in the Momotombo reservoir due to exploitation by a 2D numerical model of the system using the iTOUGH2 simulator. Particularly make an effort in calibrating the model for both single and double water equations of state to accommodate for the rapid chloride decline observed after peak production.

2. BACKGROUND

2.1 Data sources

The exploration, development and field operations of the Momotombo geothermal field were carried out by the government of Nicaragua through the National Energy Authority with the collaboration of several international institutions and cooperating countries. Substantial numbers of papers are available in the public geothermal literature. For example, the International Geothermal Association (IGA) gives access to 16 papers, and 3 papers have been published by the UNU-GTP (González B., 1990; González S., 1990; Porras, 1991). Therefore, the data available for this study come from several sources. Chemical data from the period between 1980 and 2013 were provided by Empresa Nicaragüense de Electricidad (ENEL), initially called Instituto Nicaragüense de Energía (INE). The chemical analyses were reported by Arnórsson et al. (1996) and entered into the database of ENEL. Many of the data sets of temperature, pressure, enthalpy, production, and reinjection water used in this report for the assessment of changes in the Momotombo geothermal field come from Enrique Porras' PhD dissertation (2005). Finally, the above mentioned publications in the IGA database have been carefully reviewed and used to identify topics of interest for this study.

2.2 Momotombo production history

The Momotombo geothermal field started production in 1983 when the first turbine unit of 35 MWe was commissioned. As shown in Figure 2, the power output was relatively stable at about 35 MWe from 1983 to 1986. During this time period, this unit was fed from five shallow wells (MT9, MT12, MT20, MT23 and MT27). At the end of 1986, the output started decreasing because Well MT9's casing collapsed (Porras, 2006).

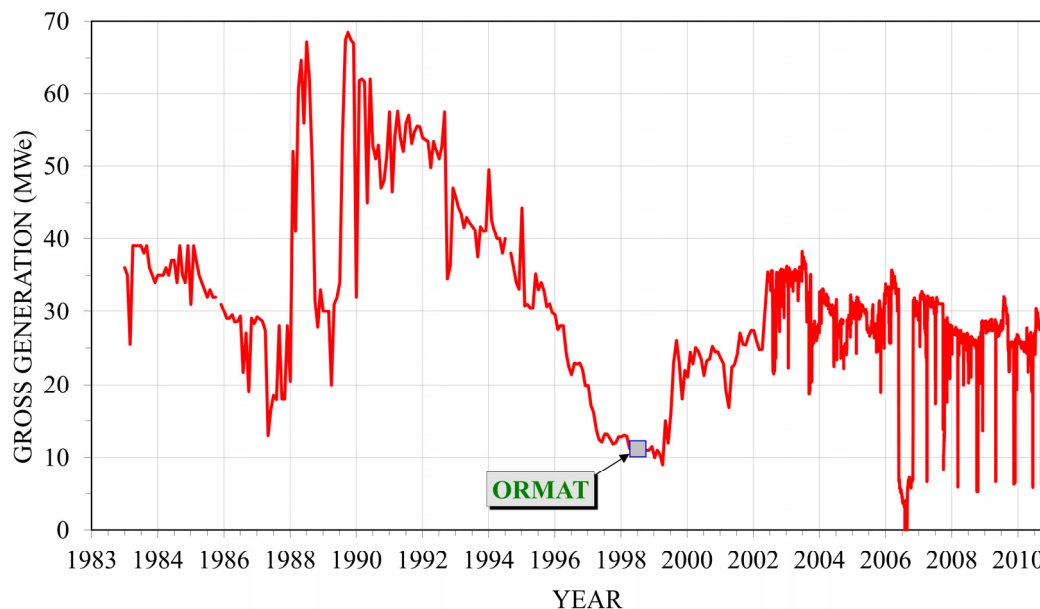


FIGURE 2: Power generation history of the Momotombo geothermal field (Porras, 2012)

Six years after the start of production, in 1989, a second 35 MWe unit was installed, tapping steam from an additional six shallows wells. When the second unit started to work, the output reached about 66 MWe for a short period, then fell back to 30 MWe because of generator and/or turbine vibrations. Also, Well MT36 dropped out of operation early after commissioning the second unit because of a high concentration of non-condensable gases in the produced steam (Porras, 2006).

The highest peak of power output, 69 MWe, was reached in 1990 after the turbine vibration issue had been resolved. However, from 1990 to 1999, the power output declined steadily to about 9 MWe (Figure 2). From 1992 until 1997, three new wells were drilled to make up for the loss in power output but, unfortunately, this effort was unable to mitigate the productivity decline of other wells.

In 1999, the power output had declined to about 9 MWe. Only 7 wells were producing, mainly because the shallow wells located in the central part of the field were damaged by scaling while other shallow production wells, located in the eastern part of the wellfield, were suffering from cooling (Porrás, 2006).

In July 1999, Ormat took over management of the field with the goal to rehabilitate the Momotombo geothermal power plant. Rehabilitation consisted of work-overs, acid stimulation, calcite scaling inhibition, repairing mechanical failures, cementing jobs, full reinjection and mitigating the cooling effect of re-injection by pushing the injected mass to the eastern wellfield boundary and, finally, drilling deep wells in order to evaluate the possibility of recovering steam production. Figure 2 shows a sizeable recovery of power output in 2000.

In 2002, an organic unit Rankine cycle Ormat Energy Converter (OEC) was commissioned with a 7 MWe installed capacity, fed by separated brine at a temperature of 155°C; the brine is cooled down to about 100°C before being reinjected. This increased the total installed capacity to 77 MWe.

In 2003, the power output peaked at 35 MWe, but then started to decline due in part to enthalpy losses arising from cold fluid intrusion into the shallow feedzone reservoir. This hampered considerably the steam and flow rates of four shallow production wells. This decrease might also have been affected by plugging; removing calcite scale after mechanical cleaning could result in skin damage in the vicinity of the well (Porrás, 2006).

The current Momotombo wellfield has 47 wells, of which 11 are for production, 7 are reinjection wells and 3 are monitoring wells. 17 wells failed and 9 are dry wells no longer producing; these were drilled during the four drilling stages (1974-1978, 1981-1985, 1992-1996 and 2000-2002). The well depths range from 300 to 2839 m (Porrás, 2005). Figure 3 shows the location of all the wells.

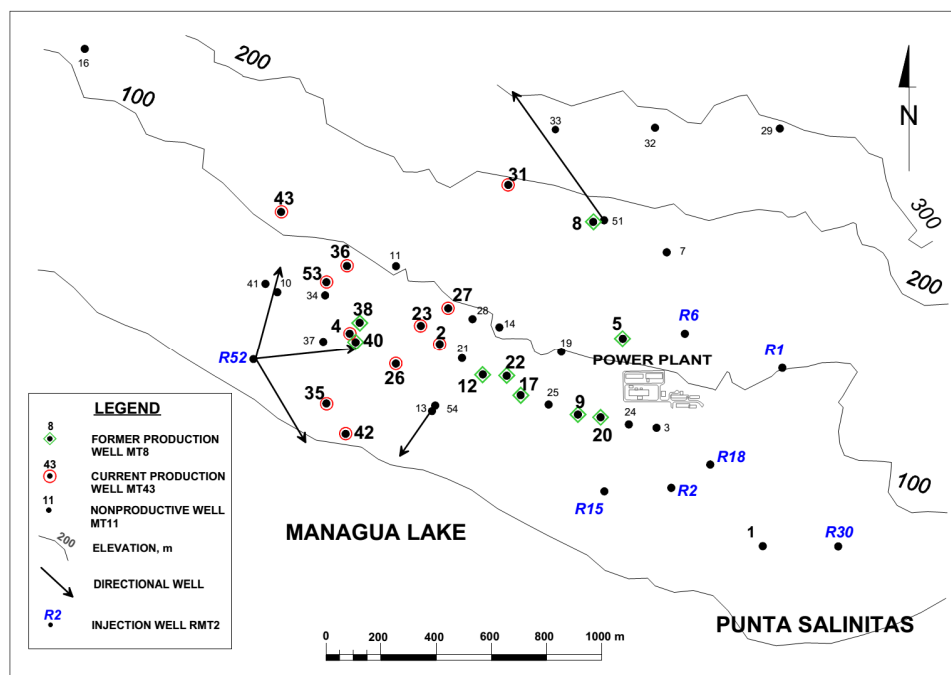


FIGURE 3: Location map of production and reinjection wells of Momotombo (Porrás and Björnsson, 2010)

Initially, the Momotombo power plant was fed by 24 production wells. Nowadays, the power plant has only 11 production wells connected. Table 1 lists the current production wells with information about their location, depth, casing depth and elevation.

TABLE 1: Current production wells in Momotombo (Porrás, 2005)

Well name	Coordinates		Depth (m)	Casing depth (m)	Elevation (m)
	East	North			
MT-2	549096	1370355	490	356	60
MT-4	548776	1370397	1435	665	74
MT-23	549027	1370428	864	260	71
MT-26	548941	1370286	640	266	49
MT-27	549126	1370486	442	368	87
MT-31	549360	1370933	582	338	202
MT-35	548686	1370235	1295	603	56
MT-36	548755	1370634	1653	650	97
MT-42	548755	1370047	2093	1420	42
MT-43	548536	1370845	2500	1682	128
OM-53	548693	1370583	2053	1103	88

Reinjection is a very important part of any geothermal development and is often a key factor in the success or failure of many power projects. Momotombo geothermal field began operating a limited reinjection system during the period 1983-1989, but the scheme has changed in terms of the magnitude of the amount of reinjection as well as the reinjection water temperature. Most of the separated water was discharged into Managua Lake until 1999. The location of the reinjection wells is shown in Figure 3 with names that start with R; these wells are located mainly in the eastern part of the well field. In this report these reinjection wells are also referred to as RMT followed by the identification number.

The separated water was sent to these wells either pressurized by pump or as gravitational flow (Porrás, 2005). Initially, the temperature of the reinjected water was 170°C, but it gradually decreased to 155°C in 2003, and is now just about 100°C after commissioning the binary unit. Figure 4 shows the histories of brine production and reinjection at Momotombo from the beginning in 1983 until 2009. We can see in the figure that the re-injected fraction increased substantially after 1999.

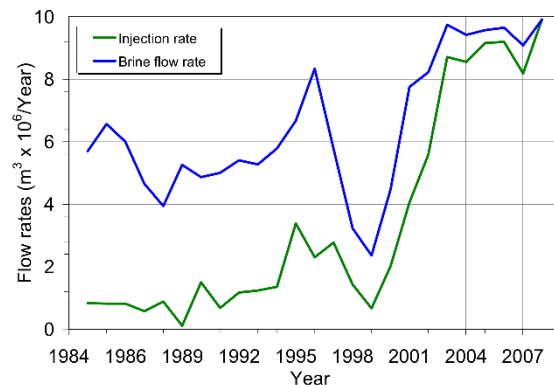


FIGURE 4: Brine production and reinjection

In 2002-2003 two tracer tests were conducted to identify the hydrological flow paths and the rate of return prior to installation of the OEC, thereby supporting a revised injection strategy for the well field. The analysed tracer tests suggested that there is a direct connection between the East wellfield and the production wells and indicates high permeability, most likely characterized by fractures in the shallow reservoir (Björnsson, 2008).

The analysis revealed that Well RMT15 has a good connection with the production wells, Well RMT6 can be used as an injector with a low risk of the production wells cooling, and that Wells RMT2 and RMT18 are good reinjection wells. A revised geological model of the field suggests a south-north boundary separating Wells RMT2 and RMT18 from the rest of the wells (Kaplan, 2004).

A new injection strategy was adopted since installation of the binary unit began in 2003, with limited injection into Well RMT15, and maximizing injection into Wells RMT2, RMT18 and RMT30.

2.3 Geological setting

The Momotombo geothermal field is located on the southwest flank of the Cordillera Los Marrabios which has several high temperature geothermal resources on the northern shore of Lake Managua at the foot of the Momotombo stratovolcano. The field was developed in the scope of the Nicaragua depression within which the Momotombo volcanic complex is located. The volcanic complex consists of several small volcanic cones and a large caldera located adjacent to and northwest of the Momotombo volcano.

The area of the Momotombo geothermal field is characterized mainly by three fault systems: NW-SE, NE-SW and N-S (Figure 5). Regional faults are aligned in a N-S direction; the Momotombo fault and the SR fault are the principal NW-SE trending faults, and in the centre part of the wellfield, the NE-SW trending Björnsson's fault is the principal fault. These sets of faults allow the circulation of fluids in a hydrothermal system. The most productive shallow wells are located in a zone corresponding to structural crossings in a fractured zone formed in the intersection of the faults of these three systems (Porras, 2009).

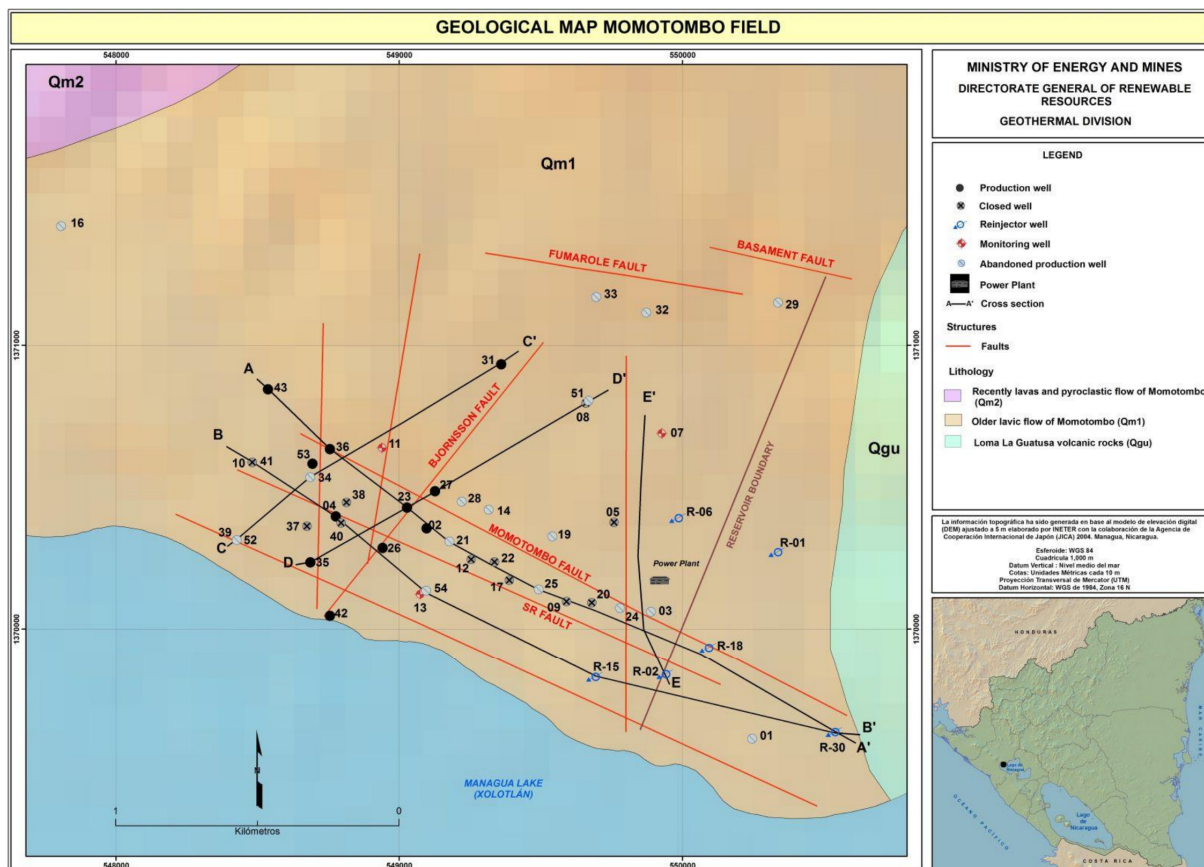


FIGURE 5: Geological map of Momotombo field (Egilsson et al., 2012)

The petrographic study by Combredet et al. (1987) showed that the lithology of the Momotombo geothermal field has been divided into the six units: unit I: 0-260 m b.s.l.; unit II: 260-600-800 m b.s.l.; unit III: 600-800 m b.s.l.; unit IV: 1600-2000 m b.s.l.; unit V: 360 m thick; and unit VI: 2300 m b.s.l. These formations consist of andesite and andesite-basaltic volcanic products, volcano-clastic deposits, different kinds of tuffs, volcano-sedimentary and sedimentary deposits, and some sub-intrusive bodies and dikes. This study suggests that a long period of volcanic activity took place in this area and that the formations were formed during early Miocene to the Quaternary age. The volcanic and volcano-clastic deposits have a total thickness of about 1700 m.

The rocks of the Momotombo geothermal reservoir consist of an interlayered sequence of lavas, tuff and pyroclastics down to a depth of 1500-1700 m and range in composition from basaltic to dacitic. Below this there are ignimbrites with minor tuffs. Light grey silty sediments underlie the ignimbrites. Andesitic dykes occur in the sediments (Arnórsson et al., 1996).

The wells in the Momotombo field are distributed in an area of about 3 km², but most of them are concentrated in an area of only 1.5 km².

2.4 The conceptual reservoir model

A conceptual model of Momotombo has been published in several articles (López et al., 1980; Porras et al., 2005; Björnsson, 2008; Porras and Björnsson, 2010). The model has not changed drastically through the years but has been refined as more data became available. The early conceptual models of the Momotombo geothermal field were developed by different consulting companies and after each exploration stage a thorough study of all technical data was generated. The 4 stages are described by Cordon (1980):

Stage 1: This model was developed by Texas Instruments in 1971. The objective was to delineate the field using geological and geophysical methods, and to confirm the presence of high temperature at depth.

Stage 2: This model was developed by the United Nations Development Program in 1973. Its most important contribution was to provide geochemical data that strongly suggested an upflow of thermal water originating in a deep and high-temperature reservoir. Sveinn S. Einarsson, then advisor to the United Nations, revised this model in 1977, based on analyses of the temperature distribution in drillholes (Einarsson, 1977).

Stage 3: The Electroconsult model was developed by Electroconsult in 1977 and isotope analyses suggested the existence of two reservoirs, in a convective cell, developing within permeable formations and some cold water inflow from the east partially feeding the shallow reservoir.

Stage 4: This model was developed by California Energy Company in 1979. This study included an analysis of temperature measurements and geological observations from 33 wells. Also, the first stratigraphic column was presented.

The IECO (International Engineering Company) model was developed from analyses of subsurface temperature distribution and from previous findings by various companies. This model found that the shallow reservoir is controlled by fracture permeability within the 200 m to 500 m depth range and that the deep reservoir extends to the west with increasing depth, but has an abrupt temperature drop near the eastern margin of the fracture zone due to cold water inflow.

The concept of two geothermal reservoirs was later applied to Momotombo, based on the depths to the production zones: one is a shallow reservoir and the other is a deep reservoir (González, 1990). There are three permeable horizons: a shallow permeable layer (200-700 m b.s.l.) and two layers located around 700-1500 and 1500-2000 m b.s.l. (Porras, 2012).

It is evident that the Momotombo field (Figure 6) is not a geothermal reservoir in which fluids are heated by conduction, but rather this field is part of a hydrothermal convective system (Goldsmith, 1980). The geothermal reservoir is hosted in andesitic flows and tuffs; the permeability of these rocks is controlled by faults and associated fracture zones. Some of these faults correspond to the lateral boundaries of the reservoir (Porras, 2005).

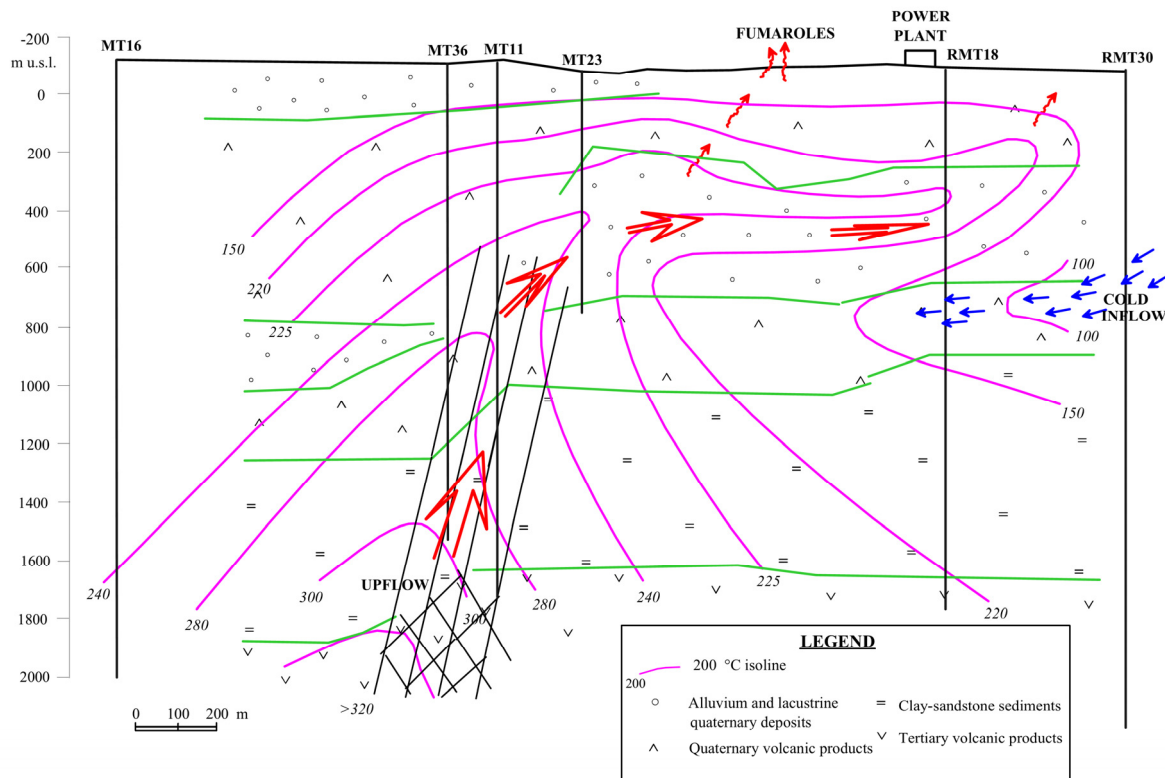


FIGURE 6: Temperature cross-section and a conceptual model of the Momotombo geothermal field (Porras and Björnsson, 2010)

The steady state condition of the Momotombo reservoir was a liquid single phase but then changed to a liquid-steam two phase reservoir soon after fluid production started in 1983. The two phase zone was developed mainly in the shallow reservoir when more fluid was produced for the second unit in 1989 (Porras, 2006).

The current conceptual model was most recently published by Porras and Björnsson (2010). This model is a review of previous models, based on information derived from deep drilling and the production history. Figure 6 shows this conceptual model as a temperature cross-section from west to east with a vertical upflow zone as a prominent feature. Most of the shallow production wells located in the middle of the field present 225-250°C feeding zones at intermediate depths. Wells drilled in the eastern part of the field encountered temperature inversions below this high temperature zone. Waters with temperatures below 100°C were found at intermediate depths, suggesting inflow (recharge) from either Lake Managua or from shallow cold water aquifers. The conceptual model is limited in that very few wells reach 500 m b.s.l., which makes the temperature distribution at deep levels less certain than at shallow levels. Geochemical studies have not conclusively determined whether Lake Managua is the source of this low-temperature inflow (Arnórsson et al., 1996). The production wells in the eastern half of the field were initially fed by a shallow lateral flow of boiling water from the major upflow (Arnórsson et al., 1996).

3. CHANGES IN FLUID CHEMISTRY WITH TIME

The dynamic production history of Momotombo is largely attributed to fast pressure and enthalpy changes resulting from up to 69 MW of steam generation from only 1-2 km² of proven wellfield. The pressure and enthalpy changes are described in detail in earlier publications (Porras, 2005). The geochemical changes, which are considerable have, however, received less attention. This chapter is

to give some highlights of these changes, later to be revisited in this study by an iTOUGH2 numerical study.

3.1 Chloride concentration history of produced fluid

The Momotombo geothermal reservoir is a sodium-chloride liquid dominated system. It has two reservoirs with an inflow of cold water from the east and an upflow of hot water from the central west. The changes observed in chemical composition between 1983 and the present are related to rapid infiltration of local and cold meteoric water into the shallow aquifer. Additionally, some of the declines in production were due to the encroachment of reinjected water into the production zone, and boiling in the reservoir as a result of extensive exploitation (Verma et al., 1996).

Chloride is amongst the most useful non-reactive chemical species used in geochemical analysis of liquid dominated geothermal reservoirs. Initially, reservoir water of Momotombo contained about 2700-3300 ppm Cl (Arnórsson et al., 1996). It is evident that chloride concentrations in many of the well discharges have changed with time, especially in the shallow wells (less than 600 m deep) in the eastern part of the production field (MT2, MT12, MT17, MT20 and MT22). Wells MT23, MT26, MT35 and MT38 are of intermediate depth (600-1300 m) and showed a moderate decline in chloride concentrations with time. Well MT36 is the deepest producing well and has maintained chloride levels the same as shallow Well MT27. Verma and Arnórsson both concluded that the decreasing chloride concentrations are caused by the incursion of cold water into the geothermal reservoir in response to the pressure loss accompanying its exploitation.

According to a report by Quijano (1989) using data from four production wells (MT12, MT20, MT23 and MT27) and hot springs near the area, chloride concentrations of springs before exploitation of the field were similar to weirbox water from the wells. This indicated that springs were a direct discharge of the reservoir. Boiling occurs at the shallower levels of the reservoir (300-500 m deep) in response to exploitation. Formation boiling also occurred at deeper levels of the reservoir where the permeability was less (Wells MT31 and MT35).

Figure 7 gives a better understanding of chloride behaviour in the reservoir with time and how it correlates to the exploitation history of the field. The figure shows how chloride concentrations

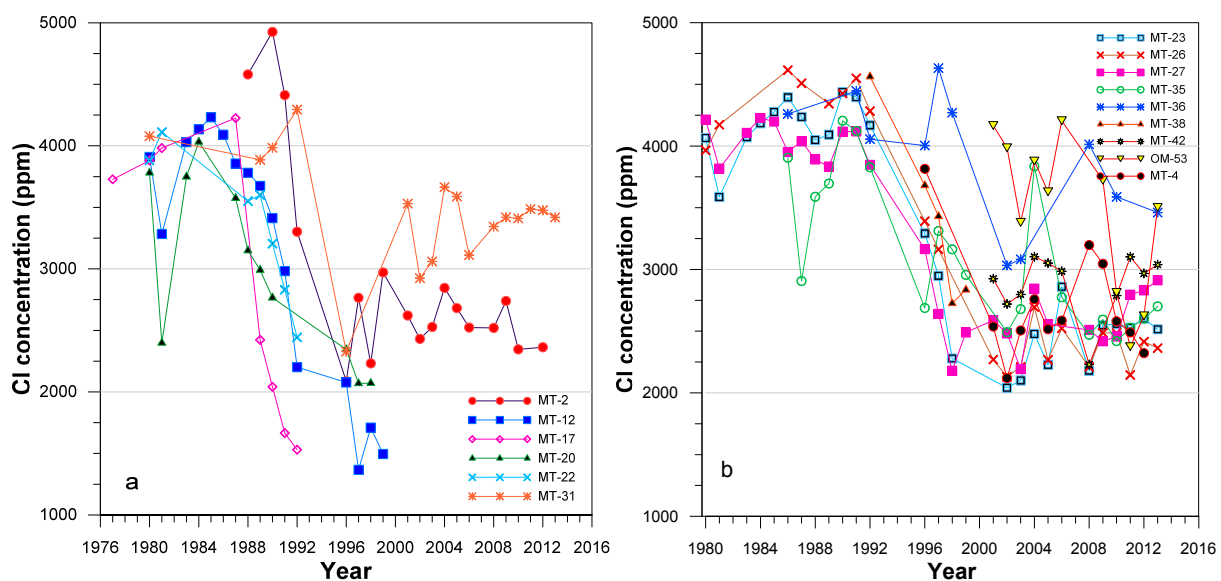


FIGURE 7: Average annual chloride concentrations: a) Cl concentrations of shallow wells located at the edge of the shallow reservoir with time; b) Cl concentrations for shallow and deep production wells located in the western part of the wellfield with time

decreased rapidly in early times, most evident in the shallow wells. Initially all the shallow wells had a chloride concentration of around 4000 ppm but this changed over time, decreasing to about 2000 ppm with the exception of the shallow wells MT2 and MT31.

Well MT31 maintained a stable concentration of chloride between 1980 and 1992. Then it experienced a decrease in concentration. In 2006 the chloride concentration reached about 3000 ppm and has remained semi stable until today. Well MT2 showed similar behaviour, with a rapid decline until 1996 and then maintained a constant concentration of chloride of about 2500 ppm.

Wells MT23, MT26 and MT27 showed relatively stable values of around or above 4000 ppm until 1992 followed by a drastic decline to values of about 2000 ppm. These wells are located on the Björnsson fault. When Well MT42 came online in 1997, it showed values of around 3000 ppm but declined to around 2000 ppm in 2008, while in 2012 it again recovered to about 3000 ppm. Well MT36 showed a constant concentration of about 4000 ppm until 2002. Wells MT4, MT35 and MT38 showed a gradual decline from around and above 4000 ppm to around 2500 ppm. Well OM53 started with a concentration of about 4000 ppm in 2001 but fluctuated around this value until 2008 and between 2009 and 2011 the concentration declined to around 2500 ppm. In 2013, Well OM53 had a chloride concentration of about 3500 ppm.

After the 1990-1996 period of rapidly declining chloride concentration, most wells reached a relatively constant value between 2000 and 3000 ppm with the exception of Wells MT31 and MT36 which had values of about 3500 ppm.

As a note of caution, this study was unable to definitely confirm if the chloride concentrations in Figure 7 are that of the reservoir or in the weir box. In the latter case, the chloride values in Figure 7 need to be converted to a slightly lower value, a task which is beyond the scope of this report.

4. MONTE CARLO VOLUMETRIC ASSESSMENT

Geothermal resource assessment is a process for estimating the amount of thermal energy that can be extracted from a geothermal reservoir, evaluating all available data from surface discharge and downhole. These data are evaluated along with other geoscientific information obtained from geological, geophysical and geochemical measurements. The main focus of this assessment is to confirm that there exists a geothermal resource and this gives a certain capacity for a certain period with well-defined fluid characteristics and resource management strategies to ensure production sustainability over a long term period (Sarmiento and Steingrímsson, 2011).

The Monte Carlo simulation is a numerical volumetric modelling technique that uses variables that are often shrouded in uncertainty, making it necessary to define a probability distribution for these variables. By using such random values for the most sensitive volumetric model parameters, a probability distribution can be assessed for the reservoir power generation capacity. The discrete distribution for the outcome is quantified or divided into intervals of proven, probable and possible reserves, giving the upside potential and downward risk in sizing up the field power potential (Sarmiento and Steingrímsson, 2008).

4.1 Thermal energy calculation

The volumetric method refers to the calculation of the thermal energy in the rock and the fluid. It is based on the volume and temperature of a reservoir. The equation used in calculating the thermal energy for a liquid dominated reservoir is as follows:

$$Q_T = Q_r + Q_w \quad (1)$$

and

$$Q_r = A * h [\rho_r * C_r * (1 - \phi) * (T_i - T_f)] \quad (2)$$

$$Q_w = A * h [\rho_w * C_w * \phi * (T_i - T_f)] \quad (3)$$

where Q_T = Total thermal energy (kJ);
 Q_r = Heat in rock (kJ);
 Q_w = Heat in water (kJ);
 A = Area of the reservoir (m²);
 h = Average thickness of the reservoir (m);
 C_r = Specific heat of rock at reservoir conditions (kJ/kgK);
 C_w = Specific heat of liquid at reservoir conditions (kJ/kgK);
 ϕ = Porosity;
 ρ_r = Rock density (kg/m³);
 ρ_w = Water density (kg/m³);
 T_i = Average temperature of the reservoir (°C); and
 T_f = Final or rejection temperature (°C).

When the reservoir has a two-phase zone, it is necessary to calculate the heat component of both liquids. A comparison made by Sanyal and Sarmiento (2005) indicates that if only water is produced from the reservoir, only 3.9% of the stored heat is contained in the fluids; the rest is in the rock matrix. If only steam is produced from the reservoir, only 9.6% is contained in the fluids. If both water and steam are produced from the reservoir, between 3.9 and 9.6% of the heat is contained. Conclusively, all the fluids are in the rock and it doesn't matter whether one distinguishes between the stored heat in the water and steam, respectively.

The possible size of a new power plant that could be supported by the resource in question is based on the following equation:

$$P = \frac{Q_t * R_f * C_e}{P_f * t} \quad (4)$$

where P = Power potential (MWe);
 R_f = Recovery factor;
 C_e = Conversion efficiency;
 P_f = Plant factor; and
 t = Time in years (economic life).

The *recovery factor* refers to the fraction of the stored heat in the reservoir that could be extracted to the surface. It is dependent on the fraction of the reservoir that is considered permeable and on the efficiency by which heat could be swept from these permeable channels. The *conversion efficiency* takes into account the conversion of the recoverable thermal energy into electricity. The *economic life* of the project is the period it takes the whole investment to be recovered within its target internal rate of return. This is usually 25-30 years. The *plant factor* refers to the plant availability throughout the year, taking into consideration the period when the plant is scheduled for maintenance, or whether the plant is operated as a base-load or peaking plant. The good performance of many geothermal plants around the world places the availability factor to be between 90 and 97 %.

The Monte Carlo simulation is used to determine the proven, probable and possible or inferred reserves based on the resulting percentiles obtained from the cumulative frequency or the probability density function, where the proven reserves will have a P90 (90 percentile) probability, P50 for the proven + probable reserves, and P10 for the proven + probable + possible reserves. The percentile value indicates the probability value that the quantity of the reserves to be covered will equal or exceed the proven reserves. The accuracy of this method depends on the type, amount and quality of

geoscientific and engineering data and the accuracy increase when the field has wells and production data become available (Sarmiento and Steingrímsson, 2008).

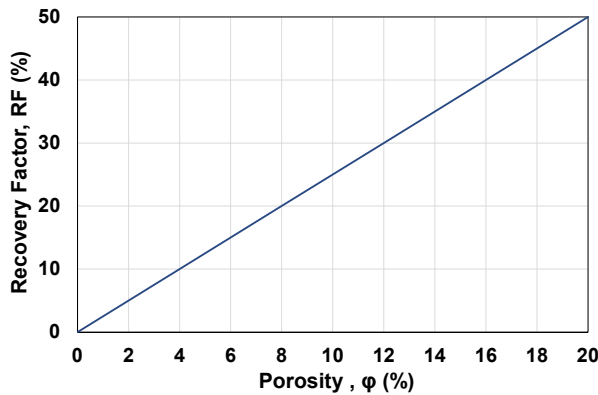


FIGURE 8: Correlation between porosity and recovery factor (from Muffler, 1979)

4.2 Recovery factor

The recovery factor cannot be measured directly, but a constant value (0.25) was often applied in earlier reservoir assessment and sometimes this is estimated to be a function of the reservoir porosity (Muffler, 1979). In Figure 8, we can see the theoretical geothermal recovery factor as a function of reservoir porosity.

Nowadays it is generally believed that the recoverable fraction of the stored energy was overestimated at least for fractured reservoirs (Williams, 2007).

4.3 Parameter evaluation

In this study, the Momotombo reservoir area was estimated by taking into account the resistivity contours, temperature contours and geophysical exploration of the current wellfield. These are used to define the proven reservoir. As there may be an existing reservoir sector still to be discovered, another scenario of double the proven resource is studied, here called the possible reservoir. The thickness of the reservoir was taken from the correlation of temperature and pressure profiles of the wells and petrographic analysis (Figure 6). The temperature of the reservoir was defined by the temperature profiles, indicating that the reservoir temperature increased in the western part of the well field, where the highest temperature above 320°C was found for Well MT43 below 2250 m b.s.l. (Figure 6). The most likely recovery factor was conservatively estimated as 15% for the calculation of thermal energy available in a volume of porous media, based on the volcanic nature of the reservoir. The 10% most likely porosity assumption will, for example, give 25% recovery, using Figure 8.

The assessment analysis of the potential of the field, using the Monte Carlo volumetric method was explained above and the parameters used in this analysis are summarized in Table 2.

TABLE 2: Parameters used to estimate probability distribution for the Monte Carlo simulation

Parameters and units	Proven (P ₉₀)			Possible (P ₁₀)			Type of distribution
	Min	Most likely	Max	Min	Most likely	Max	
Surface area (km ²)	1	2.5	3	3	5	7	Triangular
Thickness (m)	1000	2000	3000	1000	2000	3000	Triangular
Rock density (kg/m ³)		2500			2500		Single value
Porosity (%)	5	10	15	5	10	15	Triangular
Rock specific heat (J/kg°C)		900			900		Single value
Temperature (°C)	200	250	320	200	250	320	Triangular
Fluid density (kg/m ³)		799.2			799.2		f(temp)
Fluid specific heat (J/kg°C)		4870			4870		f(temp)
Recovery factor (%)	10	15	25	10	15	25	Triangular
Conversion efficiency (%)		11			11		f(temp)
Plant life (years)		25			25		Single value
Rejection temperature (°C)		150			150		Single value

4.4 Results of production capacity

The results obtained through the Monte Carlo volumetric method are shown in Figure 9 which shows the frequency distribution and the cumulative probability distribution of the proven and possible reservoir. Figures 9a and 9b indicate that the proven reservoir has a mean value of capacity of 26 MWe with a standard deviation of 11 MWe, while the most likely value of the power production capacity is 20 MWe for 25 years of plant life. We can also see that the estimated power production will be in the range of 13-41 MWe and the cumulative distribution shows that the resource capacity will be at least 10 MWe. Figures 9c and 9d indicate that the possible reservoir's estimated capacity of the Momotombo geothermal field has a mean value of 60 MWe with a standard deviation of 24 MWe, and the most likely value of the power production capacity is 50.5 MWe for 25 years of plant life. We can also see that the estimated power production will be in the range of 32-93MWe and the cumulative distribution shows that the resource capacity will be at least 40 MWe. Note that the volume of the proven reservoir is 5 km³.

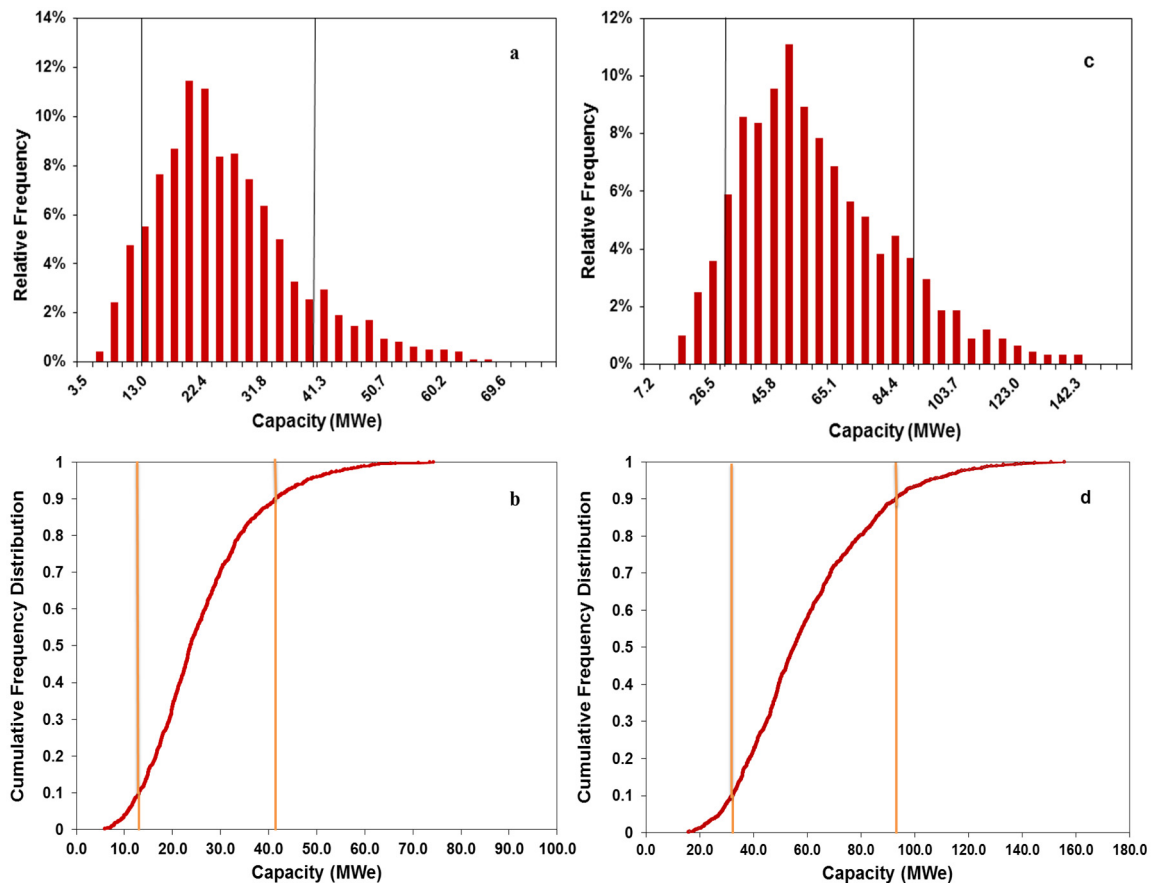


FIGURE 9: Comparison between assessment of proven and possible reserves of the Momotombo field: a) Relative frequency of power production capacity of proven assessment; b) Cumulative frequency of power production capacity of proven assessment; c) Relative frequency of power production capacity of possible assessment; d) Cumulative frequency of power production capacity of possible assessment

Comparing the proven and possible assessments, we can see that the difference is 30 MWe; this is because the values of the surface area are different. In Tables 3 and 4, the values obtained from the Monte Carlo volumetric assessment are summarized.

TABLE 3: Most likely estimate from Monte Carlo simulation

	Proven		Possible	
	Most likely	Random pick	Most likely	Random pick
Total energy (TJ)	1207	1074	2414	3900
Total recoverable energy (TJ)	181	180	362	832
Electric power	20	25	50	116

TABLE 4: Monte Carlo simulation results

	Proven	Possible
	MW _e	MW _e
Mean electric power (MWe)	26	60
Median electric power (MWe)	24	55
Standard deviation (MWe)	11	24
90% above (P ₁₀ MWe)	13	32
90% below (P ₉₀ MWe)	41	93

5. SIMPLE LUMPED PARAMETER MODEL

The lumped parameter modelling approach constitutes an efficient method of simple modelling used to simulate pressure response data from a liquid dominated geothermal reservoir and provide information on the corresponding properties of the geothermal system in question. The principal purpose of such modelling is to estimate the production potential of geothermal systems through pressure response predictions and to estimate benefits of different management options.

In simple models, the real structure and spatially variable properties of a geothermal system are greatly simplified, such that analytical mathematical equations, describing the response of the model to energy production, may be derived.

5.1 Model description

Lumped models consist of a few tanks which are connected by conductors or resistors. Fluid is produced from the innermost-tank and the pressure response to production is also monitored here. The method tackles the simulation as an inverse problem and can simulate the pressure response very accurately. It automatically fits the analytical response functions to the observed data by using a nonlinear iterative least squares technique for estimating the model parameters.

In Figure 10 we can see a general lumped parameter model; the first-tank simulates the production part of the geothermal reservoir, the second and third-tanks simulate the outer parts of the system. The

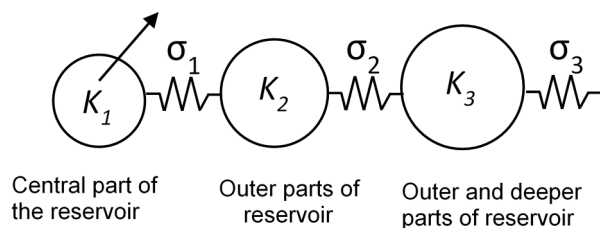


FIGURE 10: General lumped parameter model (Axelsson et al., 2005)

third-tank is connected by a resistor to a constant pressure source, which supplies recharge in the long run. Lumped models can either be open or closed. The model in Figure 10 is open; without the connection to the constant pressure source the model would be closed.

When a model is open it may be considered optimistic, since equilibrium between production and recharge will eventually always be reached

during long term production, causing the water level drawdown to stabilize. A closed model may be considered pessimistic, since no recharge is allowed for such a model and the water level declines steadily with time during long term production (Axelsson et al., 2005).

The tanks simulate the storage capacity of different parts of the reservoir in question, whereas the resistors simulate the permeability. A tank in a lumped model has the mass storage coefficient κ when it responds to a load of liquid mass m with a pressure increase by $p=m/\kappa$. The mass conductance of a resistor is given by σ when it transfers $q=\sigma\Delta p$ units of liquid mass per unit time, at a pressure differential Δp .

The basic equation describing the pressure response p of an open lumped model with N -tanks, to a constant production Q since time $t = 0$ is given by the following equation (Axelsson and Arason, 1992):

$$p(t) = - \sum_{j=1}^N Q \frac{A_j}{L_j} (1 - e^{-L_j t}) \quad (5)$$

The pressure response of an equivalent N -tank closed model is given by the equation:

$$p(t) = - \sum_{j=1}^{N-1} Q \frac{A_j}{L_j} (1 - e^{-L_j t}) + QBt \quad (6)$$

where p = Pressure (Pa);
 Q = Flow rate (kg/s);
 A_j = Coefficient of the model;
 L_j = Coefficient of the model;
 B = Coefficient of the model; and
 t = Time (s).

The coefficients A_j , L_j and B are functions of the storage coefficients of the tanks (κ_j) and the conductance coefficients of resistors (σ_j) of the model. The storage coefficient of a tank is defined by the equation:

$$\kappa = Vs \quad (7)$$

where s = $\rho_w(\emptyset C_w + (1 - \emptyset)C_r)$, storativity of the reservoir (kg/Pa m³);
 ρ_w = Density of water at specific reservoir conditions (kg/m³);
 C_w = Compressibility of geothermal fluid (Pa⁻¹);
 C_r = Compressibility of rock matrix (Pa⁻¹);
 \emptyset = Porosity of reservoir; and
 V = Volume of different tanks (m³).

One can envisage the lumped models as several concentric cylinders of radius R_i . This allows for converting the capacitors K_i to geometrically similar cylinders provided a reservoir thickness H is known. Thus:

$$R_1 = \sqrt{\frac{V_1}{\pi H}}; R_2 = \sqrt{\frac{V_1 + V_2}{\pi H}}; R_3 = \sqrt{\frac{V_1 + V_2 + V_3}{\pi H}} \quad (8)$$

Therefore:

$$r_1 = \frac{R_1}{2}; r_2 = R_1 + \frac{(R_2 - R_1)}{2}; r_3 = R_2 + \frac{(R_3 - R_2)}{2} \quad (9)$$

where R = Radius of different tanks (m);
 H = Thickness of the reservoir (m); and

r = Half radius of different tanks (m).

For one and two dimensional flow, the conductance is defined by the following equations:

$$\sigma = \frac{Ak}{Lv} \tag{10}$$

$$\sigma = \frac{2\pi Hk}{\ln(r_2/r_1)v} \tag{11}$$

where A = Flow area (m²);
 k = Permeability (m²);
 L = Length of resistor (m); and
 v = Kinematic viscosity (Pa s).

Thus, one can estimate the volume of the lumped reservoir model with Equation 7. The reservoir permeability can then, in turn, be estimated by Equations 10 or 11. Finally, with a fully calibrated model at hand, it may be used to predict the pressure changes in the reservoir in the future for given production scenarios.

5.2 Simulation results

Axelsson and Arason (1992) developed the simulation program Lumpfit to obtain pressure changes in hydrological reservoirs. This lumped model methodology was used to obtain information about reservoir properties of the Momotombo field; the model was based on the observed pressure changes resulting from the actual production history 1983-2004. In this case, the total production history was digitized from Figure 3.7 in Porras (2005). Likewise, the pressure change histories in Wells MT11 and MT13 were digitized from Figures 3.7 and 3.9 in Porras (2005) to construe a pressure response curve. In this case the total production was used instead of the net production since reinjection was insignificant until the year 2000.

The procedure for finding the best fitting parameters for a specific lumped model is as follows: in the first step a one-tank open model was used and then a two-tank open model. The results of the simulation for total production are shown in Figure 11, the model parameters are shown in Table 5 and the properties of the Momotombo reservoir are summarize in Table 6.

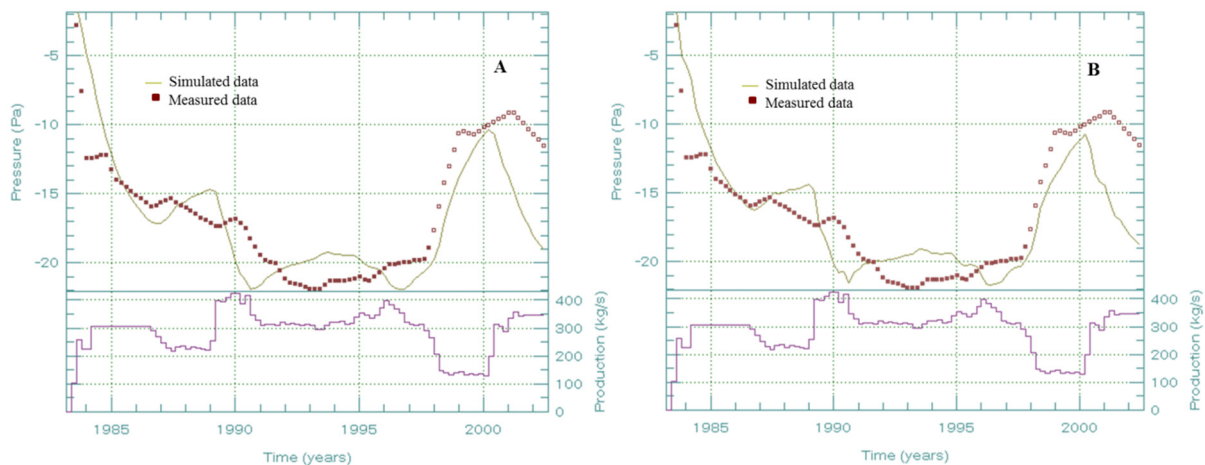


FIGURE 11: Total production and pressure response data of the Momotombo geothermal field simulated by a lumped parameter model: a) One-tank open model; b) Two-tanks open model

TABLE 5: Parameters of the simulation by lumped model

Parameters	Total production	
	Open, one-tank	Open, two-tank
A ₁	0.504570×10 ⁻¹	0.303737
L ₁	0.817232	25.9474
A ₂		0.304736×10 ⁻¹
L ₂		0.613834
B		
κ ₁ (ms ²)	6250.08	943.596
κ ₂ (ms ²)		9913.23
σ ₁ (10 ⁻³ ms)	0.161966	0.707262
σ ₂ (10 ⁻³ ms)		0.211813
Coeff.of determin. (%)	65.1	70.4
Misfit standard deviation (bars)	2.16	2.02

TABLE 6: Properties of the reservoir according to lumped model

Properties	Model	First-tank	Second-tank
Reservoir volume (km ³)	Two-tanks open	0.4	4.2
Permeability (mD)		232	75

Using a two-tank open model resulted in a satisfactory fit between the measured and simulated pressure (Figure 11b). One assumption, however, was necessary to attain this match, namely neglecting pressure data collected after 2000 when large scale injection commenced. The first-tank can be considered the innermost part of the geothermal reservoir and the second acts as the surrounding recharge area of the system.

The best fitting lumped model reveals a storage coefficient of the main area κ_1 and the recharge area κ_2 as 943.6 and 9913.2 ms², respectively. The conductivity σ_1 and σ_2 is 0.71×10^{-3} and 0.21×10^{-3} ms, respectively. Using the storativity published by Porras (2005) and Equation 7, the volume of the first-tank and the volume of the second-tank were calculated as 0.4 and 4.2 km³, respectively.

Assuming two-dimensional flow and using the most likely parameters of the Monte Carlo volumetric method (Table 2), the thickness of the reservoir is 2 km, the radius of the first-tank equals 250 m and the radius of the second tank equals 850 m. Therefore, $r_1 = 124.57$ m and $r_2 = 551.93$ m. Using Equation 11, the permeability estimated for the first tank is 232 mD and 75 mD for the second tank.

6. A 2D DISTRIBUTED PARAMETER MODEL BY iTOUGH2

The present study concludes by using the simulator iTOUGH2 (Finsterle, 1999) to calibrate a 2D vertical slice model of the Momotombo reservoir. iTOUGH2 was developed on top of the TOUGH2 (Pruess et al., 1999) simulator code for adding inverse modelling capabilities. This automates the process of repeatedly improving parameters to obtain a better fit to data and adjusts in a direction that minimizes the differences between observed and calculated values.

6.1 Governing equations

TOUGH2 is a numerical simulation program for multi-dimensional, multi-component and multi-phase flow of mass and heat in porous and fractured media. The TOUGH2 architecture is based on a model mesh that consists of a number of elements connected to each other. For each of these elements, we need to set up a number of equations defining the accumulated mass and heat, fluxes of heat and mass through all surfaces and generation points where applicable.

The governing equations of mass and heat are discretized and solved between consecutive time steps by the Newton-Raphson iteration scheme. The basic mass and energy balance equation solved by TOUGH2 has the general form (Pruess, 1999):

$$\frac{d}{dt} \int_{V_n} M^\kappa dV_n = \int_{\Gamma_n} F^\kappa \cdot n d\Gamma_n + \int_{V_n} q^\kappa dV_n \quad (12)$$

The first term (M) of Equation 12 represents mass or energy accumulation in sub-volume V , where κ can denote 1 water, 2 air, 3 heat, 4 tracer, 5 CO₂ ...etc. The second term (F) represents mass or heat fluxes through the surface of our sub-volume V and the last term (q) represents sources and sinks of mass and heat. The normal vector is denoted by n on surface element $d\Gamma_n$, pointing inward into V_n .

The mass accumulation term is specified as:

$$M^\kappa = \emptyset \sum_{\beta} S_{\beta} \rho_{\beta} X_{\beta}^{\kappa} \quad (13)$$

where M^κ = Total mass of component κ (kg);
 \emptyset = Porosity;
 S_{β} = Saturation of phase β ;
 ρ_{β} = Density of phase β (kg/m³); and
 X_{β}^{κ} = Mass fraction of component κ present in phase β .

The heat accumulation is written as:

$$M^{N\kappa+1} = (1 - \emptyset)\rho_R C_R T + \emptyset \sum_{\beta} S_{\beta} \rho_{\beta} U_{\beta} \quad (14)$$

where ρ_R = Grain density of the rock (kg/m³);
 C_R = Specific heat of the rock (J/kg °C);
 T = Temperature (°C); and
 U_{β} = Specific internal energy in phase β (J/kg).

Advective mass flux is specified as a sum over phases:

$$F^\kappa|_{adv} = \sum_{\beta} X_{\beta}^{\kappa} F_{\beta} \quad (15)$$

And individual phase fluxes are given by a multiphase version of Darcy's law:

$$F_{\beta} = \rho_{\beta} u_{\beta} = -k \frac{k_{r\beta} \rho_{\beta}}{\mu_{\beta}} (\nabla P_{\beta} - \rho_{\beta} \mathbf{g}) \quad (16)$$

where u_{β} = Darcy velocity in phase β (m/s);
 k = Absolute permeability (m²);
 $k_{r\beta}$ = Relative permeability to phase β (-);
 μ_{β} = Dynamic viscosity (kg/ms);
 P_{β} = $P + P_{c\beta}$, fluid pressure in phase β (Pa);
 P = Pressure of a reference phase (usually a gas phase) (Pa);

$P_{c\beta}$ = Capillary pressure (≤ 0) (Pa); and
 g = Vector of gravitational acceleration (m/s^2).

The heat flux contains both conductive and convective components:

$$F^{NK+1} = -\lambda \nabla T + \sum_{\beta} h_{\beta} F_{\beta} \tag{17}$$

where λ = Thermal conductivity ($W/m \text{ } ^\circ C$); and
 h_{β} = Specific enthalpy in phase β (J/kg).

6.2 Development of a 2D numerical model

As discussed in an earlier section concerning the chemistry changes in Momotombo, it is of interest to see if these can be observed in distributed parameter numerical models. Particularly, it would be good to determine the cause of the chloride concentration changes shown in Figure 7. Therefore a 2D numerical model study using the iTOUGH2 platform was conducted and is presented below.

6.2.1 Model mesh and boundary conditions

A rectangular area of 3000 m length by 2500 m depth and 200 m thickness was selected as the basis for the 2D numerical model and then adjusted to the conceptual model shown in Figure 6. The model selected has 540 elements with 11 wells and is divided into 9 rock types. In Figure 12 we can see the model mesh and the rock type distribution calibrated for iTOUGH2. The different colours mean the following: red is the basement, yellow represents the surface, green is a shallow reservoir, light blue is the vertical permeable zone feeding model hot springs on the surface, orange is a deep vertical up flow zone, blue represents cold water inflow from the east, grey is the western boundary and pink is the eastern boundary.

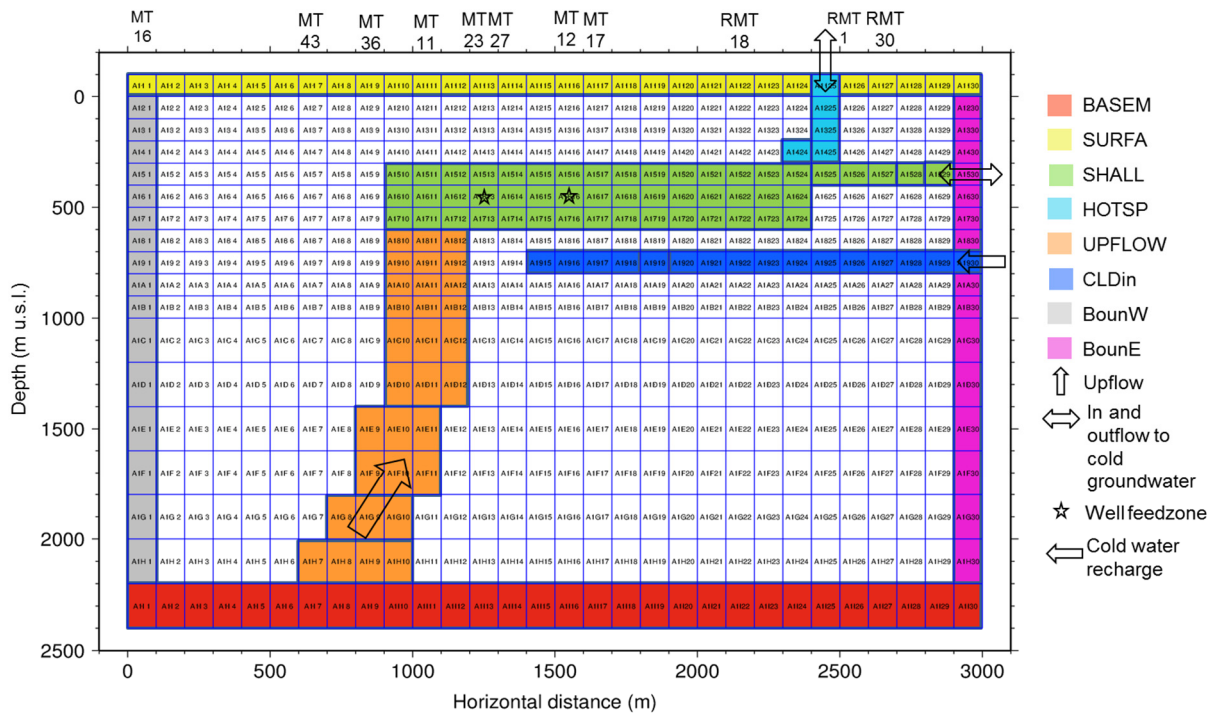


FIGURE 12: Mesh of the 2D numerical model of the Momotombo reservoir

The model's top and eastern constant pressure boundary conditions is regarded here as Lake Managua that has a chloride concentration of around 200 ppm (Parello et al., 2008). The numerical model was designed such that this low temperature lake water is able to flow into the deep model, if its pressure declines during production while discharging fluid to the surface under natural state conditions. The top, bottom, east and west boundary layers were defined as inactive; they remain at constant pressure and temperature at all times. This was actually not the case in the early model calibration, when the two outer vertical boundaries were assigned the steady state temperature profiles of Wells MT16 (BounW) and RMT30 (BounE). Their pressure could, however, change and were only set as steady state when the model pressure satisfactorily matched the observed initial pressure of Well MT11.

The top SURFA layer was centred at 50 m a.s.l. and given a fixed pressure of 4 bars and about 1 mD vertical permeability to the layer below. The bottom BASEM layer, on the other hand, was give very low vertical permeability but the temperature distribution was in line with the temperatures shown in Figure 6. Heat could, therefore, flow vertically between this base layer and the active layers above, while mass flow was negligible.

6.2.2 Sources and sinks

The 2D Momotombo model is heated by a constant mass inflow of around 1500 kJ/kg enthalpy into the deepest orange coloured upflow elements shown in Figure 12. This mass rises up to 300-500 m depth where it enters the horizontal shallow reservoir. The fluid here will move laterally to the east where two flow channels allow it to escape from the model. One is by the hot spring upflow zone called HOTSP while the other is to a constant pressure and temperature element in the 5th layer of the BounE rock column. Note that both connections deliberately allowed for either outflow or inflow, subject to the model pressure.

In addition to the mass upflow and outflow boundary conditions at the surface, only two production wells were introduced to study the model enthalpy, pressure and chloride changes with time after 1983. These were Wells MT27 and MT12. Both produce at a constant arbitrary 10 kg/s flow rate, Well MT27 from 1983, while Well MT12 was put online in 1989 when the second 35 MW unit was commissioned. This assumption greatly simplified the actual production history of the Momotombo field, but was deemed necessary and reasonable for a two month long study exercise. For those interested in a more detailed reservoir model, the PhD thesis of Porras (2005) is an appropriate reference.

6.2.3 Modelling chloride changes with time

In the present model, substantial effort was put into imitating the declining chloride concentrations of the wells with time (Figure 7). For this endeavour, the two water option of TOUGH2 was applied. The basic assumption is that the deep and hot geothermal inflow consists of 99% of water 1 while the top ground water layer is, on the other hand, 99% mass fraction of water 2. As the model execution took off, the two waters mixed in the model and their mass fractions were constantly updated by the TOUGH2 mass balance equations.

A simple linear relation was used to convert the mass fraction of water 1 to chloride concentration in ppm, namely, by multiplying the mass fraction by 4000, which is the initial chloride concentration of the deeper and hotter Momotombo wells (Figure 7).

6.2.4 Observations in calibrating the model

A total of 12 observation data sets were used in calibrating the model mesh shown in Figure 12. These grouped firstly into the initial temperature profiles in Wells MT11, 12, 17, 23, 36, 43, RMT1 and 18, and an initial pressure profile in Well MT11. These profiles were digitized from Figures 2.11 and 2.17 in Porras's (2005) PhD thesis. Secondly, the pressure drawdown history in Figure 11 was imported to

an element close to Well MT11. Thirdly, the observed enthalpy history of Well MT27 was digitized from Figure 3.4 in Porras (2005) and served as a constraint for allowing this well to temporarily flash into formation with an accompanying temporary rise in enthalpy. Last, but not least, the chloride history of Well MT27 (Figure 7) was imported to the inverse file of iTOUGH2 to see if the cold model boundary to the east and the surface hot spring would recharge fresh water to the shallow reservoir and, hence, result in declining chloride in the well with time.

6.2.5 Calibration of the model

The calibration in iTOUGH2 requires an inversion technique of numerical simulation. The first step is to make a model forward file. This file includes parameters of the different rock types, the model elements, connections, initial conditions and generation points. For the mesh generation, the inbuilt mesh maker of TOUGH2 was applied. Secondly, an inverse input file had to be developed, consisting of a parameter block which defined the model parameters to be inverted for, an observation block which defined the times when the code compared measured and computed values; this block also incorporated the measurements extracted from Porras's (2005) thesis. In this study, 14 model parameters were inverted for, 11 horizontal and vertical permeability, the cold water recharge rate to the CLDin layer (Figure 12), and the rate and enthalpy of the deep inflow. Finally, a computation block was written for controlling the numerics of the inversion. Of special convenience is the STEADY STATE SAVE feature of iTOUGH2 which allowed for matching both steady state and production date in the same execution.

The simulator automates the process of repeatedly improving the parameters to obtain a better fit with the data and adjusts these parameters in a direction that minimizes the differences between observed and calculated data. This misfit boils down to a single number called the objective function. It is the sum of the square of all residues of measured and computed values, divided with the standard deviation of each dataset.

Inverse calculations were required to adjust parameter block lists, including temperature, pressure, enthalpy and drawdown of the different elements of the grid. Block lists of observation times and values were used for calibration and a block list of computational options.

6.2.6 Rock properties

After creating the model mesh, it was necessary to assign rock properties to each element in the system. The rock properties are density, porosity, permeability, thermal conductivity and heat capacity. In Table 7, the rock properties of the mesh are summarized for the best model calibrated by the inverse method against the 12 datasets at hand.

TABLE 7: Rock properties for each grid in the system

Rock	Density (kg/m ³)	Porosity (%)	Permeability (m ²)			Thermal conduct. (W/m ² °C)	Heat cap (J/kg°C)
			k ₁	k ₂	k ₃		
Unknw	2650	0.20	1.000E-17	1.000E-15	7.749E-17	2.50	1.00E+03
SURFA	2650	0.20	10.00E-15	1.000E-14	1.013E-13	2.50	1.00E+03
BASEM	2650	0.10	1.000E-14	1.000E-35	1.000E-35	2.50	1.00E+03
UPFLO	2650	0.10	7.400E-15	5.000E-14	6.709E-14	2.50	1.00E+03
SHALL	2650	0.20	3.420E-13	1.000E-14	1.025E-13	2.50	1.00E+03
HOTSP	2650	0.20	4.300E-14	2.500E-13	1.882E-13	2.50	1.00E+03
CLDin	2650	0.20	1.450E-13	1.000E-14	5.081E-15	2.50	1.00E+03
BounW	2650	0.10	1.000E-15	1.000E-14	7.749E-17	2.50	1.00E+50
BounE	2650	0.10	1.000E-15	1.000E-14	7.749E-17	2.50	1.00E+50

Rock features are explained as follows: SURFA rock type was assigned to the top of the model and BASEM rock type was assigned to the base of the reservoir, both defined as inactive; UPFLO rock type was assigned at depth, SHALL rock type was assigned to shallow reservoir between 300 and 400 m, HOTSP rock type was assigned to the outflow of hot springs, CLDin rock type was assigned to cold recharge from east, and BounW and BounE rock types were assigned to the boundary located in the western and eastern part of the field, respectively. Note that the most productive reservoir volume, SHALL, is of 340 mD permeability and complies nicely with the 230 mD estimated in the lumped model.

6.2.7 Simulation results for natural state

The iTOUGH2 model match to the observed steady state data is shown in different graphs in this section. The initial setting of the parameters is very important because it causes remarkable changes in the simulation. One of the most important parameters is permeability; the rate at which fluid passes through the material depends on three basic factors in addition to the intrinsic permeability: porosity, density affected by temperature, and pressure to which the fluid is subjected.

In Figures 13-20, a comparison is done on measured and simulated temperature profiles of one monitoring well (MT11), five production wells (MT12, 17, 23, 36 and 43), and two reinjection wells (RMT1 and 18). Production Wells MT12, MT17, MT36 and MT23 are reasonably matched although Well MT23 showed a shallow steam zone. Well MT43 showed a result near the boiling point curve. Reinjection wells RMT1 and RMT18 showed a temperature inversion both in the field data and in the model. In Figure 21 we can see initial pressure in Well MT23 and a good match between measured and simulated pressure.

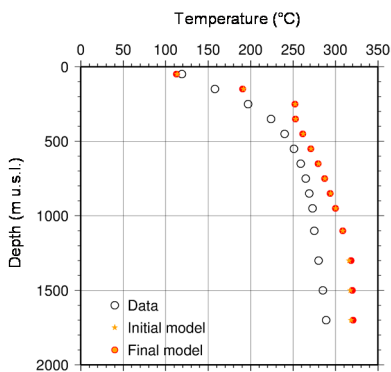


FIGURE 13: Temperature measured and simulated in Well MT11

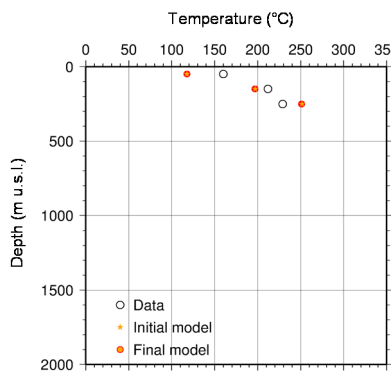


FIGURE 14: Temperature measured and simulated in Well MT12

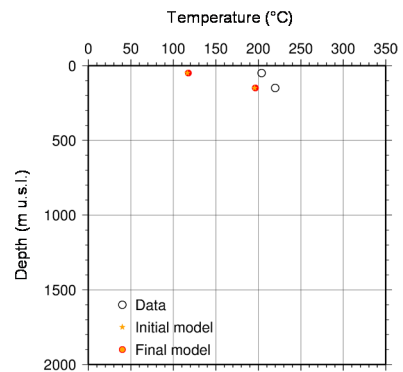


FIGURE 15: Temperature measured and simulated in Well MT17

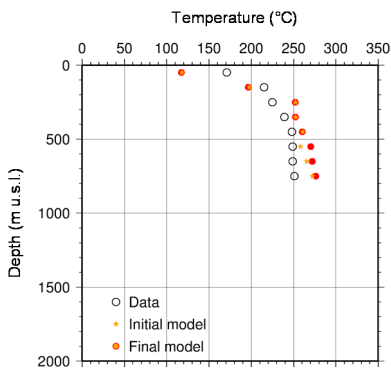


FIGURE 16: Temperature measured and simulated in Well MT23

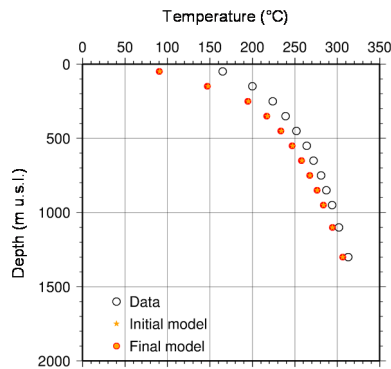


FIGURE 17: Temperature measured and simulated in Well MT36

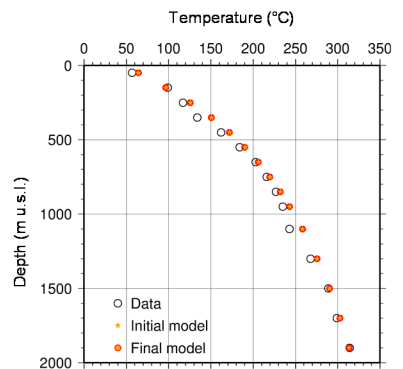


FIGURE 18: Temperature measured and simulated in Well MT43

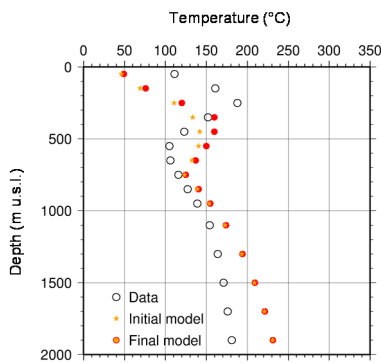


FIGURE 19: Temperature measured and simulated in Well RMT1

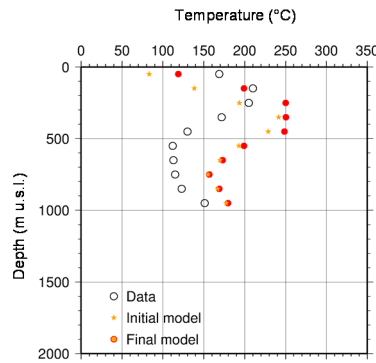


FIGURE 20: Temperature measured and simulated in Well RMT18

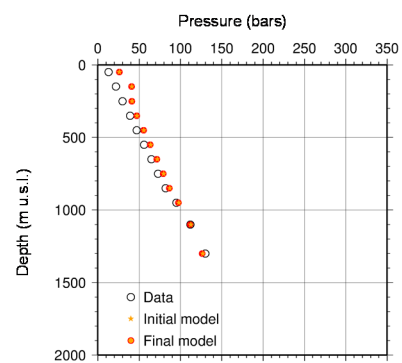


FIGURE 21: Pressure measured and simulated in Well MT23

In the natural state model, 3.3 kg/s of 1504 kJ/kg enthalpy and 330°C temperature were needed to match the temperature and pressure data presented above. The cold water lateral recharge into CLDin in the east was estimated as 0.55 kg/s of 101°C fluid.

Figure 22 presents a cross-section of the initial temperature distribution in the 2D model and the mass fraction of the deep geothermal water component in the natural state. Additionally, the graph shows that the computed model is filled by geothermal water with the exception of its shallow east corner where some free convection of the cold groundwater takes place.

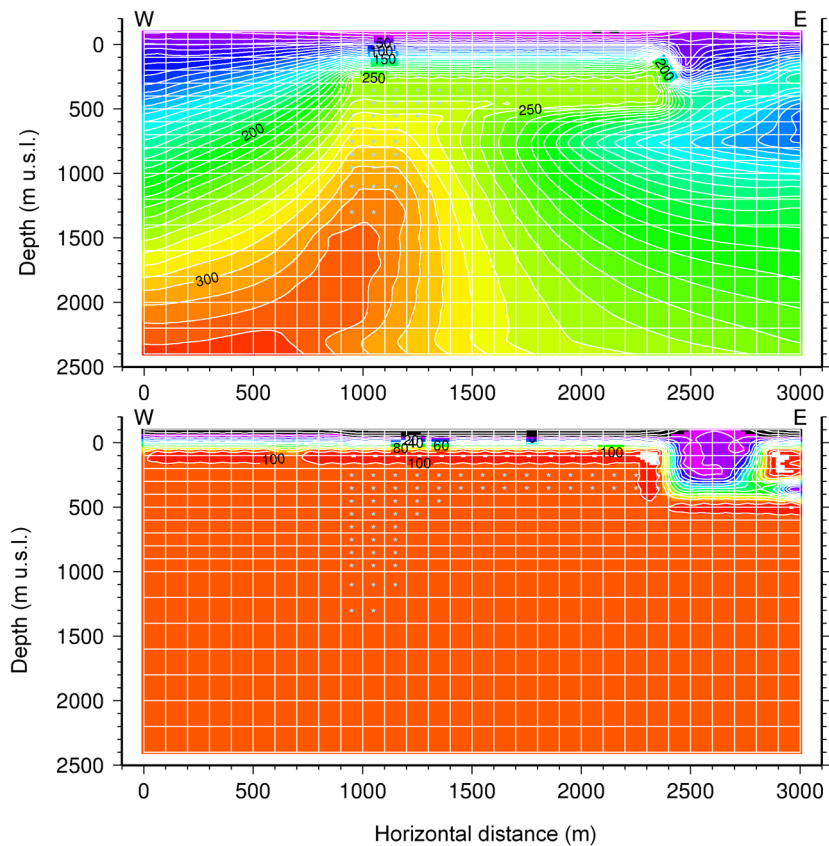


FIGURE 22: Cross-section of the initial temperature distribution and the mass fraction of the deep geothermal water component

6.2.8 Simulation results for production data

Figure 23 shows a cross-section of the final (end of year 2012) temperature distribution, mass fraction of the original geothermal water and computed reservoir cooling. A prominent feature is the invasion of fresh water from the surface near the east boundary into the shallow reservoir. It is evident that this incursion caused dilution in the chloride concentration of the production wells located in the shallow reservoir. The cross-section in Figure 23 supports the theory that many shallow wells suffer in temperature due to invasion of cold water into the reservoir.

The re-injected brine has a higher chloride concentration than the geothermal reservoir fluid and continued recirculation of the brine will result in gradually increasing the chloride concentration of the produced brine. The chloride concentration when production started was high, indicating that before the freshwater incursion started to affect the composition of the reservoir fluid, it was being affected by progressive boiling.

In Figure 24 we can see enthalpy with time of Well MT12 gradually decreasing. In Figure 25 we can see enthalpy with time of the shallow production Well MT27; when production in the second unit started, the enthalpy increased but then decreased, possibly due to fast inflow of low-temperature groundwater.

In Figure 26 we can see the pressure drawdown of the monitoring Well MT11 that is located above the upflow zone. The match between measured and simulated pressure drawdown is reasonable and can only be improved by a more thorough description of the well's flow history in a 3D model.

The chloride concentration with time was used to detect mixing of groundwater with deep recharge fluid. Decreases in the chloride concentration implied intrusion of low-temperature and low-salinity groundwater into the reservoir. Intrusion of low-temperature ground water into the reservoir and extensive boiling in the shallow reservoir due pressure drawdown induced cooling in the reservoir.

In Figure 27 we can see that the computed chloride concentration decreased with time in line with observations. This observation is, therefore, apparently of value in numerical model calibrations and should be of value in future numerical models made for Momotombo.

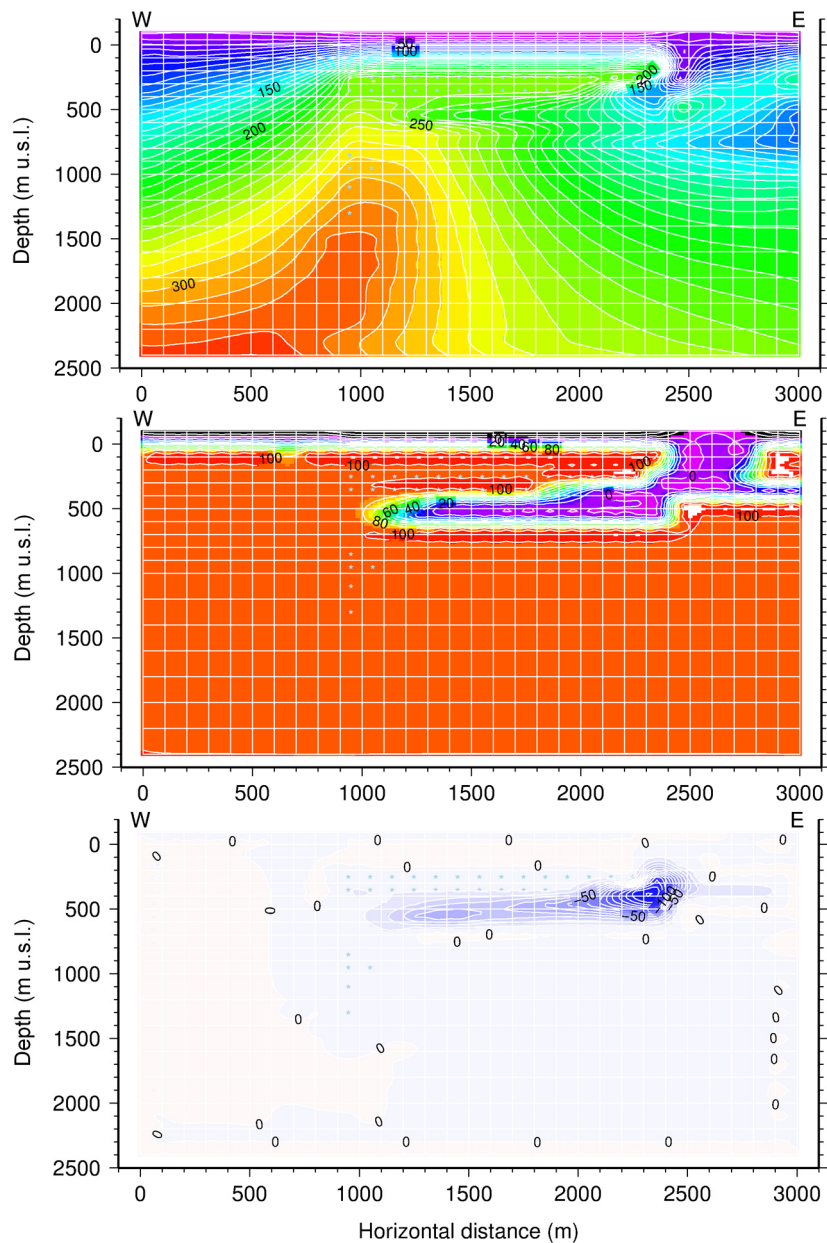


FIGURE 23: Cross-section of the final temperature distribution, mass fraction of the groundwater component and cooling model

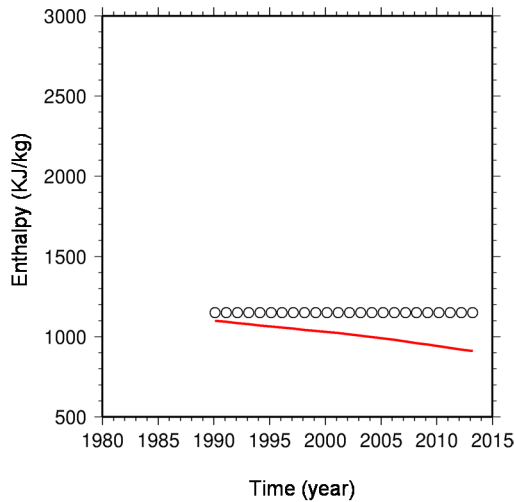


FIGURE 24: Enthalpy in Well MT12

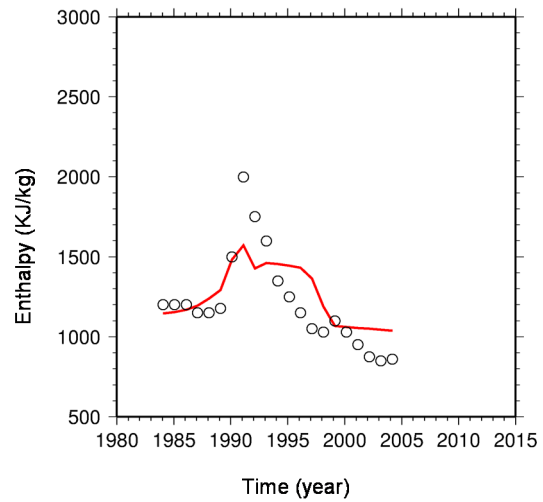


FIGURE 25: Enthalpy in Well MT-27

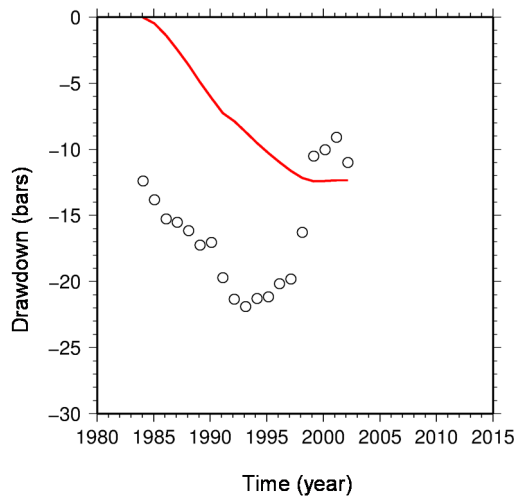


FIGURE 26: Pressure drawdown, measured and simulated, in Well MT11

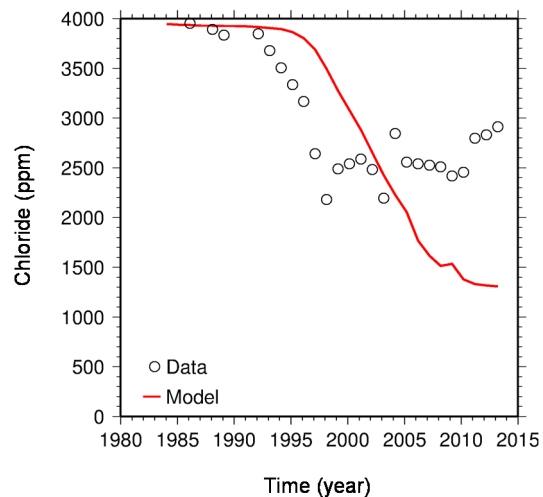


FIGURE 27: Chloride concentration in Well MT27

7. CONCLUSIONS

The main purpose of the present work was to verify the generating capacity estimates by modelling and to see if chloride changes could support the calibration of a 2D iTOUGH2 model.

The main conclusions of this work are as follows:

1. The large data base at hand allowed for simple lumped volumetric and distributed parameter numerical modeling.
2. The Monte Carlo volumetric method was used to assess the proven and possible production. The most likely values of the power production capacity is 20 MWe and 50.5 MW, respectively, for 25 years of plant life.
3. The volumetric assessment indicated that the current 30 MW production complies with the proven reservoir size.
4. More power production is a scenario only if the proven resource area can be increased.
5. The total production data and pressure drawdown could be simulated satisfactorily by one and two-tank open models.

6. The two-tank open models yielded a reservoir volume in the 4 km³ range, the same as the estimated proven reservoir volume in the Monte Carlo method. Reservoir permeability ranges from 75 to 230 mD.
7. iTOUGH2 simulation indicated that chloride concentration is a good parameter for future studies. Decreases in chloride concentration imply intrusion of low-temperature and low-salinity groundwater into the reservoir. Intrusion of low-temperature groundwater into the reservoir and extensive boiling in the shallow reservoir due pressure drawdown induced cooling in the reservoir.
8. The chloride concentration simulation infers that about half of the current reservoir fluid is diluted by cold water invasion from Lake Managua.
9. This cold fluid invasion is the primary origin of the various wellfield operational challenges faced in Momotombo.

It is recommended that a 3D model should be simulated to study the change in chloride concentration over time in all the production wells; such a model would complement the existing study by Porras (2005) while being better constrained for assessing the impact of the cold water inflow. This is a sizeable endeavor which would require man and computer power. But such a study would assist in optimizing the power production in the near future.

ACKNOWLEDGEMENTS

I want to extend my sincere gratitude to the Government of Iceland, the United Nations University Geothermal Training Programme and the Government of Nicaragua for giving me the opportunity to participate in this training. My heartfelt gratitude goes to Dr. Ingvar B. Fridleifsson and Mr. Lúdvik S. Georgsson for their support in completing this training. I also thank very much Ms. Thórhildur Ísberg, Mr. Ingimar Gudni Haraldsson, Mr. Markús A. G. Wilde and Ms. Málfríður Ómarsdóttir for their help during these six months and for making me feel welcome in Iceland. I convey my good wishes to all the lecturers and staff of Orkustofnun and ÍSOR.

Sincere thanks to my supervisor, Mr. Grímur Björnsson for being an excellent guide in the development of this report. I also want to thank Ms. Saeunn Halldórsdóttir and Dr. Gudni Axelsson for their help. Thanks so much to all UNU Fellows class 2013 for their support during the last six months, especially Claudia and Angel for their friendship, encouragement and for making this the best experience away from home.

I would like to express my appreciation to my company, Empresa Nicaragüense de Electricidad for allowing me to participate in this training and I extend my thanks to my boss, Ms. Melba Sú, for her support and confidence in me and to all my colleagues at the Geochemistry Laboratory for their valuable assistance.

Finally, I want to thank God for giving me wisdom, strength and knowledge to be able to finish my final project. Thanks to all my family, especially my mom; without your love and dedication, nothing would have been possible. Thanks, CM; love you.

REFERENCES

Arnórsson, S., Sánchez, M., Miranda, K., 1996: *Interpretation of geochemical and isotopic data from well discharges in the Momotombo Geothermal Field, Nicaragua, with recommendations on monitoring studies*. IAEA, 41 pp.

Axelsson, G., and Arason, P., 1992: *LUMPFIT, automated simulation of pressure changes in hydrological reservoirs. Version 3.1, user's guide*. Orkustofnun, Reykjavík, 32 pp.

Axelsson, G., Björnsson, G. and Quijano, J., 2005: Reliability of lumped parameter modeling of pressure changes in geothermal reservoirs. *Proceedings of the World Geothermal Congress 2005, Antalya, Turkey*, 8 pp.

Björnsson, G., 2008: Review of generating capacity estimates for the Momotombo geothermal reservoir in Nicaragua. *Geothermal Resources Council Transactions*, 32, 341-346.

Combredet, N., Guilhaumou, N., Cormy, G. and Martínez, E. 1987: *Petrographic correlation and analysis of fluid inclusions in hydrothermal quartz crystals in four wells in the Momotombo geothermal field, Nicaragua*. Instituto Nicaragüense de Energía, Managua, Nicaragua, internal report (in Spanish), 32 pp.

Cordón, U., 1980: Momotombo field models at six stages in time. *Geothermal Resources Council Transactions*, 4, 443-446.

Egilsson, Th., Halldórsdóttir, S., Espinales, A., Ruiz, F., Matus, I., Gonzalez, M., Ruiz, J., and Quintero, R., 2012: *Assessment of the Momotombo geothermal field in Nicaragua*. ÍSOR -Iceland GeoSurvey, report ÍSOR-2012/010, 225 pp.

Einarsson, S.S., 1977: Study of the temperature distribution in the geothermal reservoir at Momotombo and its implications. U.N.O.T.C. technical report NIC/74/003.

Finsterle, S., 1999: *iTOUGH2 User's guide*. Lawrence Berkeley National Laboratory, Berkeley, California, United States, Report LBNL-40040.

González B.M., 1990: *Analysis of wellbore temperatures and pressure in the Momotombo geothermal field, Nicaragua*. UNU-GTP, Iceland, report 5, 29 pp.

González S.M., 1990: *Initial temperature of Momotombo geothermal field*. UNU GTP, Iceland, report 6, 43 pp.

Kaplan, U., 2004: Geothermal cold brine injection. Two years experience in the Momotombo Field, Nicaragua. *Geothermal Resources Council Transactions*, 28, 59–64.

López, C.V., and Eckstein, Y., 1980: Six month production test at Momotombo. Preliminary results. *Geothermal Research Council Transactions*, 4, 357–360.

López, C.V., Hoyt, B.R. and Eckstein, Y., 1980: Subsurface temperature distribution and structure of the geothermal reservoir at Momotombo, Nicaragua. *Geothermal Research Council Transactions*, 4, 459–462.

Muffler, L.P.J. (editor), 1979: *Assessment of geothermal resources of the United States - 1978*. USGS Circular 790, Arlington, VA, United States, 163 pp.

Parello, F., Aiuppa, A., Calderon, H., Calvi, F., Cellura, D., Martinez, V., Militello, M., Vammen, K., and Vinti, D., 2008: Geochemical characterization of surface waters and groundwater resources in the Managua area (Nicaragua, Central America). *Applied Geochemistry*, 23, 914-931.

Porras, M.E., 1991: *Production characteristics of the Momotombo geothermal field, Nicaragua*. UNU-GTP, Iceland, report 10, 54 pp.

- Porras, E., 2005: *Development of numerical model of the Momotombo geothermal field, Nicaragua*. Kyushu University, Fukuoka Japan, PhD thesis, 207 pp.
- Porras, E., 2006: The Momotombo reservoir performance upon 23 years of exploitation and its future potential. *Paper presented at "Workshop for Decision Makers on Geothermal Projects in Central America", organized by UNU-GTP and LaGeo in San Salvador, El Salvador, 10 pp.*
- Porras, E., 2008: Twenty five years of production history at the Momotombo geothermal field, Nicaragua. *Paper presented at "30th Anniversary Workshop of the United Nations University Geothermal Training Programme", organized by UNU-GTP in Reykjavik, Iceland, 7 pp.*
- Porras, E., 2009: Geophysical exploration of the Momotombo Geothermal Field, Nicaragua. *Paper presented at "Short course on surface exploration for geothermal resources", organized by UNU-GTP and LaGeo in Ahuachapan and Santa Tecla, El Salvador, 9 pp.*
- Porras, E., 2012: Stimulating wells – The experience in the Momotombo geothermal field, Nicaragua. *Paper presented at "Short Course on Geothermal Development and Geothermal Wells", organized by UNU-GTP and LaGeo in Santa Tecla, El Salvador, 8 pp.*
- Porras, E., and Björnsson, G., 2010: The Momotombo reservoir performance upon 27 years of exploitation. *Proceedings of the World Geothermal Congress 2010, Bali, Indonesia, 5 pp.*
- Pruess, K., Oldenburg, C., and Moridis, G., 1999: *TOUGH2 User's guide, version 2.0*. Lawrence Berkeley National Laboratory, report LBNL 43134, Berkeley, CA, United States, 197 pp.
- Quijano, J.L., 1989: *Chemical and isotopic composition of the production fluids in the Momotombo field, Nicaragua*. INE, Nicaragua, internal report, 15 pp.
- Sanyal, S.K., and Sarmiento, Z.F., 2005: Booking geothermal energy reserves. *Geothermal Resource Council Transactions, 29, 467-474.*
- Sarmiento, Z.F., and Steingrímsson, B., 2008: Computer programme for resource assessment and risk evaluation using Monte Carlo simulation. *Paper presented at "Short course on Geothermal Project Management and Development", organized by UNU-GTP, KenGen, DGSM, in Entebbe, Uganda, 11 pp.*
- Sarmiento, Z.F., and Steingrímsson, B., 2011: Resource assessment I: Introduction and volumetric assessment. *Paper presented at "Short course on Geothermal Drilling, Resource Development and Power Plants", organized by UNU-GTP and LaGeo, in Santa Tecla, El Salvador, 15 pp.*
- Verma, M.P., Martínez, E.M., Sánchez, M., Miranda, K., Gerardo, J.Y., and Araguas, L., 1996: Hydrothermal model of the Momotombo geothermal system, Nicaragua. *Proceedings of the 21st Workshop on Geothermal Reservoir Engineering, Stanford University, Stanford, CA, United States, 29–34.*
- Williams, C.F., 2007: Updated methods for estimating recovery factors for geothermal resources. *Proceedings of the 32nd Workshop on Geothermal Reservoir Engineering, Stanford University, Stanford, CA, United States, 7 pp.*